Variable-Temperature Microcrystal X-ray Diffraction Studies of Negative Thermal Expansion in the Pure Silica Zeolite IFR

Luis A. Villaescusa,† Philip Lightfoot,† Simon J. Teat,‡ and Russell E. Morris*,†

Contribution from the School of Chemistry, University of St. Andrews, Purdie Building, St. Andrews KY16 9ST, United Kingdom, and the Synchrotron Radiation Source, CCLRC Daresbury Laboratories, Warrington, Cheshire WA4 4AD, United Kingdom

Received March 12, 2001. Revised Manuscript Received April 18, 2001

Abstract: Variable-temperature single-crystal X-ray diffraction using a synchrotron X-ray source has allowed the mechanism of negative thermal expansion in the pure silica zeolite IFR to be studied in greater detail than was previously possible over the temperature range 30−557 K. The results have allowed the changes in average atomic position with temperature to be measured and the structural features that are important in negative thermal expansion to be identified. The structure of zeolite IFR can be split into two regions: columns of fused rings that expand with temperature and the intercolumn regions, which tend to contract on heating. These competing changes combine to produce a material that contracts parallel to the crystallographic *a* and *b* axes and expands in the *c*-direction. Correlations between zeolite structure and thermal expansivity are also reported.

Introduction

A negative thermal expansion (NTE) material is defined as one that reversibly contracts on heating.[1] This phenomenon, which is not as unusual as was once thought, is generally caused by a structural effect (e.g. relative rotation of coordination polyhedra) that works to counterbalance and override the natural thermal expansivity of chemical bonds. Sleight and Evans have recently led a resurgence of interest in negative thermal expansion materials with the discovery of ZrP_2O_7, ZrW_2O_8, and $Sc_2(WO_4)_3$ and further developments on materials with the NASICON structure.[2−5] At the same time, research into the thermal behavior of microporous materials has revealed that they are a family of solids where NTE is the norm rather than the exception. The microporous materials most studied are the aluminosilicate zeolites and aluminum phosphates (AlPOs). Commercial applications of zeolites, such as their use in catalysis, depend critically on the structure and behavior of these materials at high temperature. Park et al.[6] were the first to record the coefficient of thermal expansion for MFI (ZSM-5), DOH (dodecasil 1H), DDR (decadodecasil 3R), MTN (dodecasil 3C), and AFI (AlPO-5).[7] For each of the materials studied there was a limited temperature range where thermal contraction was observed. Na-zeolite X has also been found to contract by Couves et al.,[8] as has Zeolite A by Colantuano.[9] However, this is believed to be due to a partial structure collapse rather than a true NTE effect like those seen in other types of solid. Siliceous faujasite and AlPO-17 have both been identified by Sleight and Attfield as exhibiting NTE,[10] AlPO-17 exceptionally so with a linear coefficient of thermal expansion (CTE) of -11.7×10^{-6} K^{-1}. This value is significantly more negative (i.e. the most contracting) than that previously reported for any material. Workers in this laboratory have also seen strong negative thermal expansion in a number of other zeolites, such as MWW,[11] ITE,[11] STT,[11] CHA,[12] IFR,[12] ISV,[13] and STF,[13] using neutron and powder X-ray diffraction. In parallel with these experimental measurements, computer simulations by Tschaufeser et al.[14] and Gale[15] have suggested that many other zeolites and AlPOs will show a negative CTE.

Detailed mechanistic information is not available for many of the systems named above, and is especially lacking for the microporous materials. Where such details are available, a number of features have been identified as contributing to the NTE effect, including the cooperative motions of "rigid" polyhedra (known as "rigid unit modes" or RUMs) and transverse vibrations of two-coordinated oxygen atoms.[1]

Single-crystal X-ray diffraction is the structural chemist's most important tool for obtaining accurate and precise informa-

* Address correspondence to this author. E-mail: rem1@st-and.ac.uk.
† University of St. Andrews.
‡ Daresbury Laboratories.

(1) Evans, J. S. O. *J. Chem. Soc., Dalton. Trans.* **1999**, 3317.
(2) Korthuis, V.; Khosrovani, N.; Sleight, A. W.; Roberts, N.; Dupree R.; Warren, W. W. *Chem. Mater.* **1995**, *7*, 412.
(3) Evans, J. S. O.; Mary, T. A.; Vogt, T.; Subramanian, M. A.; Sleight, A. W. *Chem. Mater.* **1996**, *8*, 2809.
(4) Evans, J. S. O.; Mary, T. A.; Sleight, A. W. *J. Solid State Chem.* **1998**, *137*, 148.
(5) Woodcock, D. A.; Lightfoot, P.; Ritter, C. *Chem. Commun.* **1998**, 107.
(6) Park, S. H.; Grosse-Kunstleve, R. W.; Graetsch H.; Gies, H. *Stud. Surf. Sci. Catal.* **1997**, *105*, 1989.
(7) The International Zeolite Commission identifies zeolite structure types with three-letter codes. The names relating to specific materials, rather than just a general structure type, are given in brackets. Further information can be found in: Meier, W. M.; Olson, D. H.; Baerlocher, C. *Atlas of Zeolite Structure Types*; Elsevier: New York, 1996.
(8) Couves, J. W.; Jones, R. H.; Parker, S. C.; Tschaufeser P.; Catlow, C. R. A. *J. Phys. Condens. Matter* **1993**, *5*, 329.
(9) Colantuano, A.; Dal Vecchio, S.; Mascolo G.; Pansini, M. *Thermochim. Acta* **1997**, *29*, 659.
(10) Attfield, M. P.; Sleight, A. W. *Chem. Mater.* **1998**, *10*, 2013.
(11) Woodcock, D. A.; Lightfoot, P.; Wright, P. A.; Villaescusa, L. A.; Diaz-Cabanas, M.-J.; Camblor M. A. *J. Mater. Chem.* **1999**, *9*, 349.
(12) Woodcock, D. A.; Lightfoot, P.; Wright, P. A.; Villaescusa, L. A.; Diaz-Cabanas, M.-J.; Camblor M. A.; Engberg, D. *Chem. Mater.* **1999**, *11*, 2508.
(13) Lightfoot, P.; Woodcock, D. A.; Maple, M. J.; Villaescusa, L. A.; Wright, P. A. *J. Mater. Chem.* **2001**, *11*, 212.
(14) Tshaufeser P.; Parker, S. C. *J. Phys. Chem.* **1995**, *99*, 10609.
(15) Gale, J. D. *J. Phys. Chem. B* **1998**, *102*, 5423.

10.1021/ja015797o CCC: $20.00
Published on Web 05/16/2001

tion on the structure of a material. Unfortunately, it is quite common in preparations of microporous materials for any single crystals produced to be too small for conventional laboratory single-crystal X-ray diffraction to be successful. For some time now, powder diffraction has been the only method open to investigators who need to undertake a full crystallographic study when large single crystals are not available. However, the synchrotron radiation source (SRS) at Daresbury has recently commissioned a new instrument (Station 9.8)[16] designed to perform single-crystal X-ray diffraction on extremely small crystals (this technique is called microcrystal X-ray diffraction). The promise that microcrystal diffraction holds is best illustrated with reference to some recent work, completed by ourselves, where this technique was successful in yielding the correct structure of various complex molecular sieves when other methods were unsuccessful. In this work, we have solved the structure of SSZ-23, the first zeolite with nine-tetrahedral pore openings,[17] a completely novel type of microporous material containing a macrocycle complex incorporated into the framework[18] and the structures of a number of other interesting materials.[19] It should be noted that because of the complexity of most of these materials it is unlikely that they could have been solved using any other method.

As well as small crystals, the other factor limiting interpretation of the results from diffraction experiments on zeolites is the presence in many cases of compositional disorder in the framework, which necessarily complicates the average atomic positions that are the results of such experiments. The fluoride method of zeolite synthesis, however, has provided an excellent route to the preparation of purely siliceous zeolite frameworks (i.e. pure SiO_2), where there is no compositional disorder in the framework. In addition, the purely siliceous materials are relatively free of connectivity defects, again leading to the possibility of a nondisordered material.[20] In many cases, single crystals of a suitable size for microcrystal diffraction at a synchrotron source can be prepared in this way. One such purely silica zeolite is IFR (also known as ITQ-4, Figure 1).[21] The as-made material (i.e., that still containing the organic structure directing agents and fluoride ions) shows the remarkable effect of noncentrosymmetric ordering of the organic hosts in the structure, despite the fact that the calcined IFR framework itself is centrosymmetric.[22] The structure of calcined IFR (i.e., where the template and fluoride have been thermally removed) was originally solved from powder X-ray diffraction,[21] and showed the framework topology to be centrosymmetric (monoclinic space group *I*2/*m*). The framework structure consists of small $[4^3 5^2 6^1]$ cages (i.e., cages bounded by three four-membered rings (4MR), two 5MRs, and one 6MR, Figure 2). Two of these cages are fused together via one shared 4MR (Figure 3) and these cage pairs are linked together in the *c*-direction by 6MRs to form columns. The columns are linked together by 4- and 6MRs to produce a unidimensional channel system delimited by twelve-membered-ring windows.

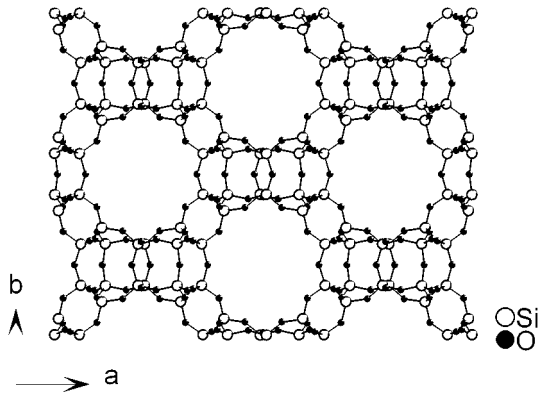

Figure 1. The structure of zeolite IFR viewed parallel to the 12-membered-ring channels.

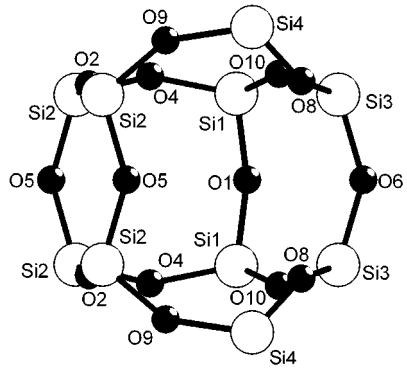

Figure 2. One of the $[4^3 5^2 6^1]$ cages from the IFR structure with the atom numbering scheme.

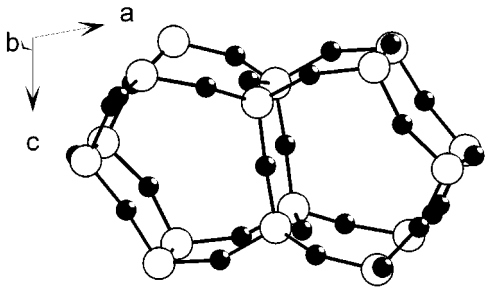

Figure 3. Two $[4^3 5^2 6^1]$ cages fused through a 4MR.

Powder X-ray and neutron diffraction experiments have been run to measure the extent of NTE.[12] These experiments were carried out on a Stoe in-house X-ray diffractometer (Cu Kα radiation), and two neutron diffractometers (Gem and Osiris) at the CCLRC Rutherford Appleton Laboratory. This work confirmed that between 50 and 550 K the unit cell volume decreases with an *average* volume coefficient of thermal expansion of -9.1×10^{-6} °K^{-1}, with individual average unit cell axis coefficients of $\alpha_a = -11.5 \times 10^{-6}$ K^{-1}, $\alpha_b = -7.47 \times 10^{-6}$ K^{-1}, and $\alpha_c = +7.19 \times 10^{-6}$ K^{-1} for *a*, *b* and *c*, respectively (where α_l is defined as $\Delta l/l\Delta T$, and *l* is the axis length and *T* the temperature). An interesting feature of this work is the contraction of the *a* and *b* axes on heating, but the expansion of *c*, which is the direction of the channels in IFR. However, at higher temperatures IFR begins to contract in the *c*-direction also. From the powder diffraction experiments, no definitive information on the mechanism of the NTE in IFR could be gleaned. In this paper we report a variable-temperature

(16) Cernik, R. J.; Clegg, W.; Catlow, C. R. A.; Bushnell-Wye, G.; Flaherty, J. V.; Greaves, G. N.; Hamichi, M.; Burrows, I.; Taylor, D. J.; Teat, S. J. *J. Synchrotron Radiat.* **1997**, *4*, 279.

(17) Camblor, M. A.; Diaz-Cabanas, M.-J.; Perez-Pariente, J.; Teat, S. J.; Clegg, W.; Shannon, I. J.; Lightfoot, P.; Wright, P. A.; Morris, R. E. *Angew. Chem., Int. Ed. Engl.* **1998**, *37*, 2122.

(18) Wragg, D. S.; Hix G. B.; Morris, R. E. *J. Am. Chem. Soc*. **1998**, *120*, 6822.

(19) Noble, G. W.; Wright, P. A.; Lightfoot, P.; Morris, R. E.; Hudson, K. J.; Kvick, Å.; Graafsma, H. *Angew. Chem., Int. Ed. Engl*. **1997**, *36*, 81.

(20) Camblor, M. A.; Villaescusa L. A.; Díaz-Cabañas, M.-J. *Top. Catal*. **1999**, *9*, 59.

(21) Barrett, P. A.; Camblor, M. A.; Corma, A.; Jones, R. H.; Villaescusa, L. A. *Chem. Mater*. **1997**, *9*, 1713.

(22) Bull, I.; Camblor, M.; Villaescusa, L. A.; Wright, P. A.; Teat, S. J.; Lightfoot P.; Morris, R. E. *J. Am. Chem. Soc* **2000**, *122*, 7128.

microcrystal X-ray diffraction experiment on zeolite IFR to attempt to determine this mechanism in more detail.

Experimental Section

Samples of purely siliceous IFR were prepared from fluoride-containing media using benzylhydroxyquinuclidinium ($BQol^+$) cations as templating (structure directing) agents to give as-made materials of formula $Si_{16}O_{32}{\cdot}F{\cdot}C_{14}H_{19}(OH)N$. The products contained small crystals (approximately $20 \times 20 \times 10$ μm^3) that were suitable for microcrystal X-ray diffraction studies. The $BQol^+$ cations and fluoride ions were removed by carefully heating the crystals at 1 deg min^{-1} to 600 °C under flowing oxygen. The integrity of the crystals remained intact after the calcination.

Single-crystal X-ray diffraction experiments were then carried out at the CCLRC Synchrotron Radiation Source, Daresbury Laboratories, UK, using the microcrystal X-ray diffraction station 9.8 equipped with a Bruker AXS diffractometer with a CCD detector. Thirteen data sets were collected between 30 and 557 K. The low-temperature data (30−90 K) were collected using an Oxford Cryosystems Helix liquid helium cryostream. The data between 100 and 350 K were collected in a stream of N_2 from an Oxford Cryosystems liquid nitrogen cryostream, and the high-temperature data (350−557 K) were collected using a thermostream hot air heater. The unit cells from these data collections agreed in their trends with those from the powder data reported earlier. However, because of the differences in absolute values obtained between the two methods, both the single-crystal and powder unit cells for each temperature were used in the refinements. There were no qualitative differences between the results in terms of trends in atomic positions. The models were refined against the diffraction data using standard least-squares refinement methods. The wavelength used in the experiments was around 0.69 Å (it varied slightly between visits to the synchrotron X-ray source). Details of the data collection and refinement results are given in the Supporting Information.

Using the high-quality data from the intermediate temperature range and the atomic positions from ref 21 as a starting model led to excellent refinements. The cooling of the crystals in the stream of cold He, even when accomplished very slowly and carefully, led to a slight deterioration in the quality of the single crystals. Heating to the higher temperatures reported here resulted in some softening of the glue and glass used to mount the crystals. This led to some difficulty in centering the crystal in the X-ray beam and in keeping it centered throughout the data collection. Both these effects resulted in the very low and very high temperature refinements being of slightly less precision compared to those in the intermediate temperature range. However, the atomic positions, and hence bond distances and angles, followed the same trends as those from the better refinements, although the precision and accuracy are worse for the high-temperature data. Thermal displacement parameters also followed the same trends, although in the low-temperature case some weak restraints were required to ensure that the tensors did not become nonpositive definite. This is due not only to the slightly poorer quality of the crystal used but also the geometric restrictions of the Helix cooling system, which leads to a slight paucity of data.

Magic angle spinning (^{29}Si) NMR experiments were conducted at the EPSRC solid-state NMR service at the University of Durham between 190 and 420 K. These showed no significant changes in ^{29}Si chemical shift with temperature.

Results and Discussion

Variable-temperature powder X-ray and neutron diffraction experiments indicated that IFR contracts on heating between about 50 and 550 K. In the temperature range accessible in the single-crystal experiments the thermal contraction is anisotropic in nature, with the magnitudes of *a* and *b* decreasing and *c* increasing with temperature (Figure 4). The evolution of Si−O bond distances with temperature follows the expected trend seen in crystallographic studies that the measured distance decreases slightly. Although this is counterintuitive since interatomic distances in bonds are known to increase, it can be explained

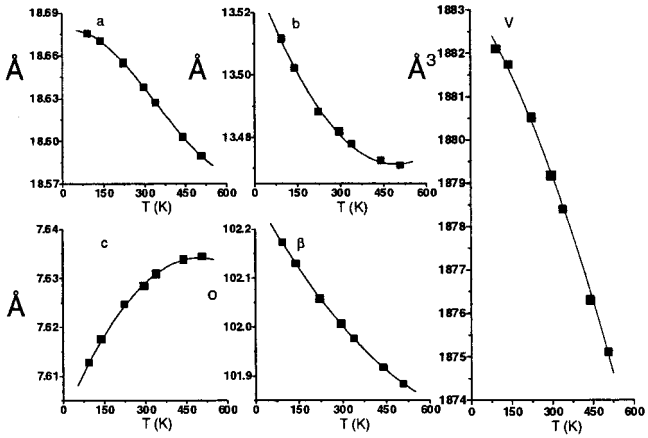

Figure 4. The thermal evolution of the lattice parameters between 50 and 550 K from powder diffraction.

by taking into account the thermal displacement parameters, which cause this observed "shortening" of the bonds. Correcting the observed distances using well-known formulas[23] leads to an increase in Si−O bond distance with temperature, although it is a very small increase over the whole temperature range. Direct measurement of the "real" thermal expansivity of Si−O bond lengths in silica by neutron diffraction indicates that this effect is even smaller than that usually obtained from corrected X-ray distances of the kind we have used.[24] The O−Si−O bond angles show no significant variation with temperature, which seems to indicate that the SiO_4 tetrahedra present in the structure can be regarded as relatively rigid units. Further confirmation of this is given by the variable-temperature MAS NMR experiments. The ^{29}Si chemical shift in zeolites is known to correlate well with the average O−Si−O bond angles in a structure.[25] In the case of zeolite IFR there is no significant change in chemical shift as the temperature is increased, indicating that the average bond angles around silicon do not change. This in itself does not imply rigid tetrahedra (an average can of course remain constant even if the sample changes its values) but it is consistent with the rigid units seen in the diffraction experiments. For a rigid unit, not only must the bond angles not change, but the atoms must vibrate in phase with each other, resulting in the mean-square displacement amplitudes of the atoms along the interatomic vectors being equal. Indeed, a thermal motion analysis carried out using the program THMA11[26] indicates that the mean-square displacement amplitudes along the oxygen−oxygen interatomic vectors are equal for each of the oxygens present in one SiO_4 tetrahedron within the experimental errors. Thus the anisotropic displacement parameters are also consistent with fairly rigid tetrahedra.[27]

One of the important factors in previous studies of NTE materials has been the transverse vibrations of two coordinated atoms. All the oxygen atoms in zeolite structures are two coordinated, and transverse vibrations of these atoms can outweigh the expansion of individual Si−O bonds and lead to a decrease in the distance between the two Si atoms connected to the same oxygen atom. There are 10 crystallographically

(23) Downs, R. T.; Gibbs, G. V.; Bartelmehs, K. L.; Boisen, M. B., Jr. *Am. Miner*. **1992**, *77*, 751.
(24) Tucker, M. G.; Dove, M. T.; Keen D. A. *J. Phys. Cond. Matter*. **2000**, *12*, 425.
(25) Thomas, J. M.; Klinowski, J.; Ramdas, S.; Hunter, B. K.; Tenakoon, D. T. B. *Chem. Phys. Lett.* **1983**, *102*, 158.
(26) Trueblood, K. N. *Acta Crystallogr*. **1978**, *A34*, 950.
(27) Dunitz, J. D.; Maverick E. F.; Trueblood, K. N. *Angew. Chem., Int. Ed. Engl*. **1988**, *27*, 880.

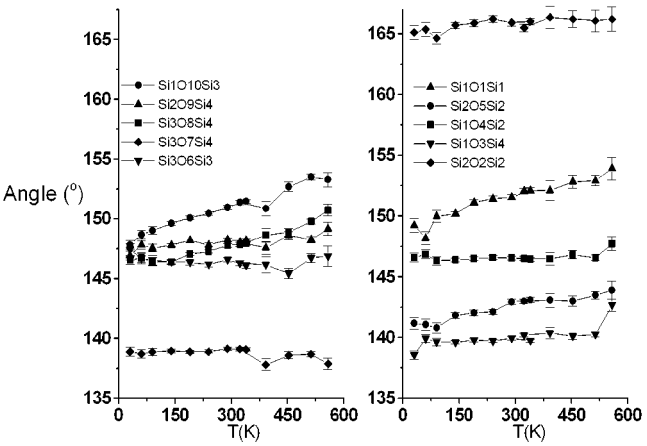

Figure 5. The variation of the Si−O−Si bond angles in the IFR structure with temperature.

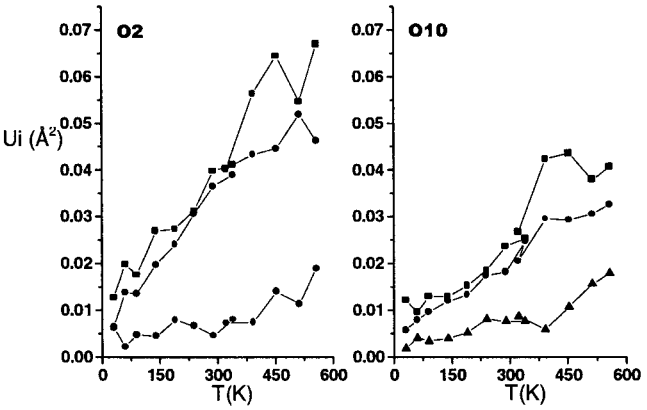

Figure 6. Plot of the principal mean square atomic displacements (principal axes of the thermal displacement ellipsoids) for O2 and O10 against temperature. The differences between the "disk"-like behavior of O2 with two large values and one small versus the "cigar"-like behavior of O10 are clearly seen. All the oxygen atoms except for O2 have "cigar"-like ellipsoids. The Si−(O10)−Si distance is the one in the structure that expands by the greatest amount, the Si−O(2)−Si distance the one that contracts the most.

independent Si−O−Si links in the structure, with four of the Si−Si distances increasing slightly with increasing temperature and six Si−Si distances decreasing over the temperature range. Interestingly, when looking at the Si−O−Si bond angles (Figure 5) it can be seen that none of the angles decrease to any significant extent, even when the effect on the angles of the corrected Si−O bond distances is taken into account. All the decrease in Si−(O)−Si distance is due to the dynamic vibration of the oxygen atoms. This is most clearly seen in the case of the Si2−O2−Si2 unit, in which the Si2−Si2 distance decreases more than any other in the structure. However, the Si2−O2−Si2 bond angle remains essentially constant over the whole temperature range. The anisotropic displacement factors for O2 are relatively large compared to those of the other oxygen atoms in the structure (Figure 6) and the resulting thermal ellipsoid is "disk"-like in nature, with two large and approximately equal principal axes of displacement, in contrast to the other oxygen atoms that have more "cigar"-shaped thermal displacement ellipsoids. This difference in vibrational behavior between O2 and the other oxygen atoms is surely related to the fact that the absolute value of the Si2−O2−Si2 bond angle is ∼15° larger than the other nine Si−O−Si angles (which range from about 140° to 150°), perhaps making it more flexible. The Si2−Si2

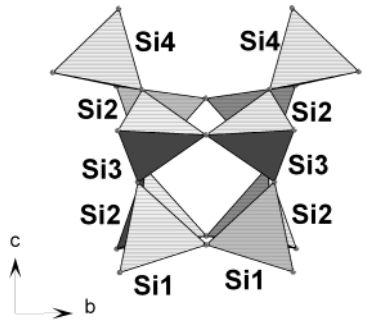

Figure 7. Polyhedral view of one of the $[4^3 5^2 6^1]$ cages in the IFR structure showing the directions of the rotations in the structure. The central silicon atoms of all the tetrahedra are labeled.

is also, as would be expected, the longest Si−(O)−Si distance in the structure.

Similar behavior of the Si−O−Si angles to this has been seen in the zeolite CIT-5 when studied by neutron powder diffraction, although the changes in angle are much less marked for IFR than in CFI (CIT-5).[13] As in IFR, none of the bond angles decrease with temperature. CFI, however, is a zeolite that expands with increased temperature and the expansion was explained in terms of the increase of a number of Si−O−Si bond angles that were in the correct orientation to produce expansion in the required directions. In the case of IFR, the Si−O−Si angles that increase the most are those including O1, O5, O8, and O10. However, only the angles containing O10 and O8 can have any contribution to the expansion along *c* as the other two angles are almost perpendicular to this axis. Significantly, the Si2−O2−Si2 unit is actually almost parallel to the *c*-axis, and it is the Si2−Si2 distance that *decreases* the most in the structure. The conclusion drawn from these results is that, unlike CFI, the expansion along the *c*-axis cannot be described as being "driven" by increases in individual Si−O−Si angles. The thermal behavior of IFR must then be explained by looking at cooperative motions (i.e. twisting) of the SiO_4 tetrahedra and the flexibility of larger units in the structure.

For descriptive purposes the structure of IFR can be split into two main parts, the relatively dense columns of fused $[4^3 5^2 6^1]$ cages that run parallel to the *c*-axis and the 4MR and 6MR units that connect these columns into the three-dimensional network. Measurement of the variation of torsion angles in the structure shows that the largest degree of twisting of neighboring tetrahedra occurs in those that make up the 5MRs (containing Si1, Si2, Si3, Si2, and Si4) in the $[4^3 5^2 6^1]$ cage.

The movement of these tetrahedra causes the average position of the atoms to alter in such as way as to force the Si4 atoms, which form the apex of the 5MR, nearer the plane containing Si1, Si2, and Si3. This plane is almost parallel to the *ac* plane of the unit cell. This results in the Si4 tetrahedra being closer together in the *b*-direction and contributing to the contraction in this direction (despite the fact that the individual Si2−O5−Si2 distance, for example, actually *increases* in this direction). The 5MR becomes more coplanar, which necessarily increases the distance from its base to its apex in both the *a*- and *c*-directions. The overall effect of this shift in the position of the Si4 atoms is most clearly seen in Figures 7 and 8. The fused-$[4^3 5^2 6^1]$ cages are linked together by 6MRs to form columns that run parallel to the *c*-axis. As the Si4 atoms move nearer to parallel with the *ac* plane (Figure 8), the 6MR linking the $[4^3 5^2 6^1]$ cages becomes more elongated in the *c*-direction and narrower in the *b*-direction.

The overall effect of the twisting of tetrahedra in the 5MR is to increase the size of the columns in both the *a*- and

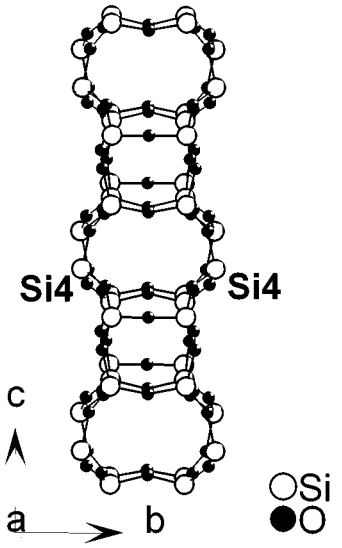

Figure 8. A view of one of the columns in the IFR structure showing the effect of the movement of Si4 (shaded atoms) on the size of the 6 rings connecting the $[4^3 5^2 6^1]$ cages in the *c*- and *b*-directions.

c-directions, and to cause a small decrease in size of the column in the *b*-direction. In total this leads to an overall increase in the volume taken up by the column part of the structure. This is not too surprising as regions containing cages should be more rigid than those comprising only single rings (such as four-membered rings and six-membered rings) and might be expected to behave more like a dense silica phase and so expand with temperature.

The increase in size of the columns in the *c*-direction can account for most of the thermal expansion of the structure as a whole seen in that direction. However, the slight decrease in size of the column in the *b*-direction and the increase in size in the *a*-direction in no way accounts for the overall decrease in unit cell dimensions measured in these directions. The overall NTE effect must them come from changes in how the columns are linked together. Figure 9 shows how the columns of fused-$[4^3 5^2 6^1]$ cages are linked together by single 4MR and single 6MR. The 4MR is relatively rigid, with almost no change in its dimensions with temperature. However, because of the movement of the Si4 atoms, which form part of both the 5MR in the cage and the 4MR linking the columns, the 4MR does reorient so that the plane of the 4MR is more parallel to the *c*-axis. This reflects the increased size of the column in that direction. The 6MR on the other hand is much more flexible, with rotations of tetrahedra and changes in individual Si−O−Si bond angles combining to reduce the distance between the columns, as measured by the Si1−Si1 distance shown in Figure 9. The variation of the component of the Si1−Si1 distance parallel to the *a*-direction correlates with the change in unit cell parameter to give a straight line with a slope of ∼0.8 (Figure 9a). Therefore, the decrease in width of each single 6MR linking the columns can account for all of the decrease in the unit cell (and a little more). However, two such Si1−Si1 distances contribute to the NTE effect per unit cell. Just taking into account the change in this distance would give a decrease in size of the *a*-axis of ∼0.27 Å over the measured temperature range. However, this is offset somewhat by the increase in the column size in this direction (∼0.075 Å per column, with two columns contributing per unit cell).

The overall effect then on the length of the *a*-axis (a decrease of about 0.12 Å over the measured temperature range) is then

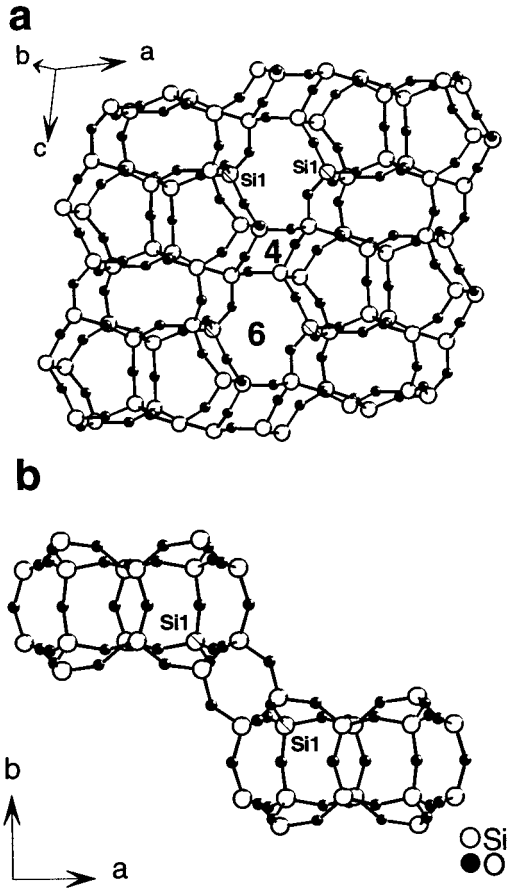

Figure 9. (a) View of the 4MR (4) and 6MR (6) units that link two columns together in IFR. (b) End view of two columns and the 4MR and 6MR units that link them. The Si1 atoms discussed in the text are labeled and shaded.

a result of two competing changes: a thermally induced expansion in the size of the columns and a contraction in the distance between the columns. There are no competing thermally induced changes in the *b*-direction. The size of the column decreases slightly parallel to the *b*-axis (Figure 8) and the component of the Si1−Si1 distance parallel to *b* decreases substantially. The variation of this component correlates with the length of the *b*-axis giving a straight line with a slope of 2.21, indicating that each Si1−Si1 distance accounts for about 45% of the total decrease (calculated from the inverse of the slope), the final 10% resulting from the decrease in the size of the column. The individual decreases are therefore additive and result in a decrease of the *b*-axis of about 0.07 Å.

As well as an overall decrease in the *a*- and *b*-axis lengths and an increase in *c*, the monoclinic angle, β (the angle between *a* and *c*), decreases with temperature. This is a natural follow-on from change in the relative positions of the columns, caused by the motions of the atoms described above.

The important feature of zeolites is, of course, their porous nature. IFR is described as having unidimensional pores parallel to *c*, with the windows delimiting the pores consisting of 12 tetrahedra (i.e., it is a 12MR channel). Since most zeolite applications involve adsorption of molecular or ionic species into the internal pores, changes in the size of the 12MR with temperature have the potential to provide very subtle control over these adsorption processes. The 12MR window to the channels in IFR is slightly puckered and is almost, but not exactly, perpendicular to the *c*-axis (Figure 10). The variation in distances across the windows is shown in Figure 11. It is

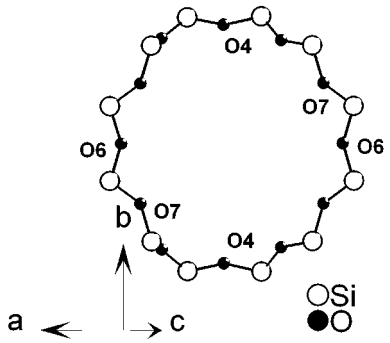

Figure 10. The 12MR window in IFR that defines the entrances to the pores. The oxygen atoms used to define the size of the window are labeled.

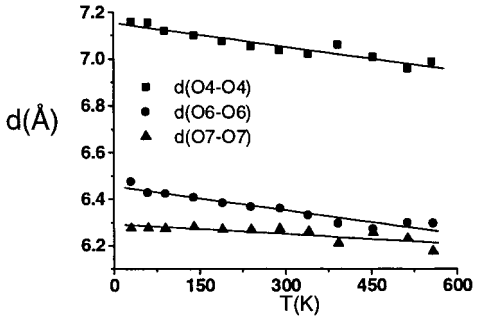

Figure 11. The evolution of the diameter of the 12MR window with temperature. The oxygen atom radius has been taken as 1.35 Å.

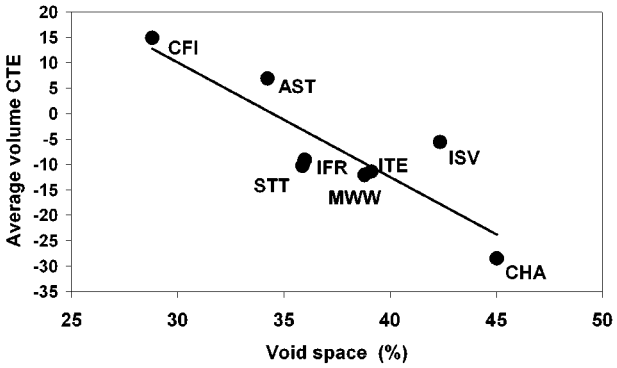

Figure 12. The correlation between volume of the void space and average volume coefficient of thermal expansion (CTE).

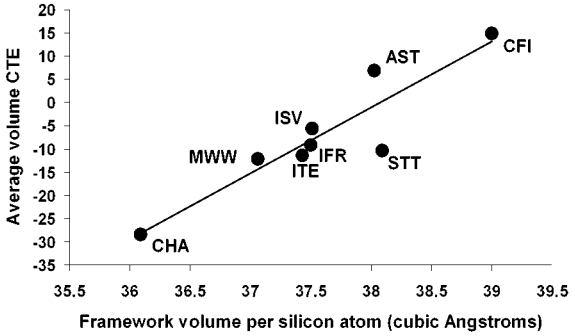

Figure 13. The correlation between framework volume per silicon atom and average volume coefficient of thermal expansion (CTE).

clear that in all directions there is a decrease in the diameter of the windows by between 2 and 3%. This could lead to a decrease in the area of the window of up to 6%, which could, in principle, significantly affect the adsorption properties of the zeolite. This might be especially useful when one considers that as the pore size of a zeolite such as IFR decreases with temperature, the size of any adsorbant molecules will no doubt be slightly increasing with temperature, the two effects being complementary.

The thermal behavior of zeolite-IFR illustrates nicely how different regions of the structure affect the thermal expansion properties of the material. The three-dimensional columns of cages are relatively rigid, and do not contribute as much to the negative thermal expansion of the material as the two-dimensional single six-membered rings that link the columns together. In general terms then, one should expect to see a correlation between the negative thermal expansion properties of a zeolite and the amount of void space present in its structure. This is somewhat intuitive, as the more space there is in a structure the easier it should be for cooperative rotations of tetrahedra to "collapse" the framework. The amount of void space present in a material can be measured in a number of ways. In this paper we have chosen to define void space as any void space large enough to accommodate small solvent molecules such as water, and calculated using the program PLATON.[28] This is not the same as the void space measured by absorption experiments, because the calculations include all void space and not only that accessible from the exterior of the material. Figure 12 shows this correlation and that it fits relatively well for most of the siliceous zeolites measured previously. It is interesting to note that two materials, ISV and AST, contract less (or expand more in the case of AST) than would be predicted simply on the basis of void space. However, these are the only structures so far measured to contain double four ring (D4R) units.

These very small 3D cages are inevitably constrained to be very inflexible, and despite the central space of the D4R being included in the calculated void space, the structure of the D4R is rigid, acting more like a small part of a dense phase such as quartz, and impeding NTE. A slightly better correlation is obtained if we plot the "framework volume" (defined as the volume of the unit cell minus the void space volume) per silicon atom versus the average volume coefficient of thermal expansion (Figure 13).

From these correlations we can conclude that the general features of zeolites that contribute to large negative thermal expansion are large void space volumes and relatively small framework volumes. Another way of looking at the framework volume is as a measure of the "thickness" of the silica walls of the channels. The thicker the walls, the more rigid, and therefore more expanding, the structure and vice versa. Therefore CHA, which has a three-dimensional pore system (and hence a large pore volume) coupled with a small framework volume per silicon atom (i.e. thin walls), shows large negative thermal expansion. CFI, on the other hand, has a unidimensional channel structure (relatively small pore volume) and a large framework volume per silicon atom giving rise to relatively thick walls.

Conclusions

Microcrystal X-ray diffraction experiments have provided us with an accurate probe of the changes in atomic position and thermal displacement parameters. This has allowed us, for the first time, to take a close look at the changes in the structures of zeolites as the temperature is varied for a fairly complex zeolite, IFR. The results show that the model of cooperative rotations of fairly rigid tetrahedra is a reasonable one for this zeolite, and that changes in unit cell parameters cannot be

(28) van der Sluis, P.; Spek, A. L. *Acta Crystallogr.* **1990**, *A46*, 194.

explained simply by changes in individual Si−O−Si angles, unlike that previously reported for CFI, in which thermal expanisivity is positive along all crystallographic axes.

The thermal properties of IFR can be described as the competitive expansion of relatively rigid columns and the contraction caused by decreasing distance between the columns, leading to overall contraction in two dimensions and expansion in one. The effect of the variation in unit cell size is to decrease the size of the openings to the 12MR channels in IFR significantly.

General correlations between the void space or framework volume per silicon atom and the thermal behavior of zeolites have been identified. However, it should be remembered that the thermal expansivity of these zeolites is often very anisotropic and sometimes quite nonlinear in nature. The thermal properties of a zeolite will depend on what temperature range the compound is studied under. Therefore simple correlations as described above will never tell the whole story, and have only limited uses as predictive tools. However, they do seem valid as a first indication of what thermal behavior is likely for a siliceous zeolite.

Negative thermal expansion effects are, of course, phonon driven and are therefore inherently anharmonic affects. Single-crystal X-ray diffraction experiments of the type described here use harmonic anisotropic displacement parameters to model vibrational motion in these materials, and so are somewhat limited in the way they can be used to explain NTE effects. However, combination of the accurate changes in average atomic position with temperature measured by X-ray difffraction with other information on anharmonic effects (from experiment or modeling) will lead to an even greater understanding of this fascinating phenomenon.

Acknowledgment. This work was funded by the Engineering and Physical Sciences Research Council. R.E.M. thanks the Royal Society for the provision of a University Research Fellow. We also thank David Apperley at the ESPRC solid state NMR service in Durham, UK for the MAS NMR measurements. We thank Oxford Cryosystems Ltd. for loan of one of their Oxford Helix open flow helium systems for this work.

Supporting Information Available: Details of representative structural refinements (CIF). This material is available free of charge via the Internet at http://pubs.acs.org.

JA015797O